Polarization-multiplexed multifocal arrays by a π-phase-step modulated azimuthally-polarized beam

Haoran Ren, Xiangping Li, and Min Gu*

Centre for Micro-Photonics, Faculty of Science, Engineering and Technology, Swinburne University of Technology, P.O. Box 218, Hawthorn, Victoria 3122, Australia

**Corresponding author: mgu@swin.edu.au*

Abstract

We demonstrate a polarization-multiplexed multifocal array capable of individually manipulating the focal polarization state in each focal spot. Breaking the rotational phase symmetry through adding a π-phase-step to an azimuthally-polarized beam leads to a linear focal polarization state with high polarization purity. Through the superposition of such modulated azimuthal polarization fields at the back aperture of the objective, multifocal arrays with individually-controllable and non-identical polarization states can be achieved. In addition, this approach exhibits a sub-diffraction-limited feature with an improved lateral resolution of 10% reduced full width at half maximums in each linearly-polarized focal spot. Consequently, applying this technique to parallel polarization-multiplexed optical recording is demonstrated.

As one of its fundamental aspects, light can selectively interact with anisotropic materials through its polarization states [1], which provides a basic principle of modern electro-optic devices. In this context, polarization microscopy [2-6] capable of manipulating the focal polarization states to tailor the light matter interaction has enabled the rapid development of polarization related applications including harmonic generation [7, 8], multi-dimensional optical data storage [9-11], single-molecule imaging [12, 13] and so on. Meanwhile, a high numerical aperture (NA) of the objective to focus the polarized beam is an essential not only for a high resolution governed by the diffraction limit [14] but also for the flexibility of focal polarization manipulation [15]. In addition to the degraded polarization purity associated to the depolarization effect, polarization microscopy enabled by a high NA objective suffers from the low throughput of such optical systems [2, 3].

On the other hand, parallel optical microscopy [16-19] through dynamic phase modulation enabled by the combination of the vectorial Debye diffraction theory and a spatial light modulator (SLM) has allowed for the generation of intensity-tunable and diffraction-limited two-dimensional (2D) [16, 17] and three-dimensional (3D) [19] multifocal arrays under a high NA objective for orders of magnitude increased throughput. Even though multifocal arrays with identical linear or cylindrical polarization states can be generated [16, 17, 19], creating polarization-multiplexed multifocal arrays with non-identical polarization states has never been

demonstrated. Therefore, it still remains a compelling challenge to further advance the multifocal array technique in polarization-multiplexed applications.

In this Letter, we report on the first demonstration of generating a polarization-multiplexed multifocal array under a high NA objective where the transverse polarization state in each focal spot can be individually manipulated. We show that the superposition of a π-phase-step filter with an azimuthally-polarized beam breaks the rotational phase symmetry in the transverse plane [20] and leads to the generation of a linearly-polarized focus oriented along the phase-step line. Thus, the superposed complex fields of multiple π-phase-step modulated azimuthally-polarized beams (π-PMABs) at the back aperture of the objective enables one to individually manipulate the polarization state in each focal spot in a multifocal array.

The principle of focusing an azimuthally-polarized beam and a π-PMAB is shown in Figs.1 (a) and 1(b), similarly, the π-phase-step can be introduced in a linearly-polarized beam for optimized confinement of its longitudinal focal field [21]. By adding a π-phase-step filter to an azimuthally-polarized beam, the field component orientated along with the phase-step line can interfere constructively. Consequently, a sharp linearly-polarized focal field with the polarization direction in parallel to the phase-step line rather than a wide doughnut-shaped azimuthally-polarized focal field (Fig. 1(a)) can be produced in the focal plane (Fig. 1(b)). Therefore, rotating

the π-phase-step filter can tune the orientation of the linear polarization of the focal spot. As such, arbitrarily-orientated transversely-polarized linear focal polarization states can be achieved.

To achieve a polarization-multiplexed multifocal array in the focal plane, the phase modulation $\phi(x,y)_i$ of each individual focal spot consists of two independent parts: aπ-phase-step filter for the focal polarization manipulation and a 2D grating function for spatially shifting the focal spot. Superposing multiple such spatially shifted π-PMABs at the back aperture of objective allows for a polarization-multiplexed multifocal array wherein each focal polarization state can be individually manipulated:

$$\Phi(x,y) = \arg\left[\sum_{i=1}^{N} w_i \exp(i\phi(x,y)_i)\right] \qquad (1)$$

where $(x,y)$is the coordinates at the back aperture plane, $w_i \exp(i\phi(x,y)_i)$ is the complex field of a π-PMAB for the ith focal spot with the phase distribution of $\phi(x,y)_i$ and a weighted amplitude of w_i, and N is the total foci number. As such, the polarization-multiplexed multifocal array can be easily achieved through a single phase-only modulator owing to the superposition principle in Eq. (1). To enable high intensity uniformity, the vectorial Debye diffraction theory [3] is used to evaluate the intensity distribution in the focal region and the uniformity can be adaptively adjusted through the weighted amplitude w_i , defined as : $w_i^n = \sqrt{w_i^{n-1}[\sum_{i=1}^{N} abs(E(x_i^f, y_i^f)/M * abs(E(x_i^f, y_i^f))]}$ ($w_i^0 = 1$), in Eq. (1) [19, 22]. For the experimental implementation, the phase modulation for a polarization-multiplexed multifocal

array is displayed in a SLM (Holoeye Pluto, 1080×1920 pixels, 256 gray levels) and relayed to the back aperture of a high NA objective (Olympus, 100×, UPLSAPO, 1.40 NA) through a 4f telescope, as illustrated in Fig. 1(c).

To demonstrate the capability of individually-controllable non-identical focal polarization states in a multifocal array, parallel fluorescence imaging of single gold nanorods was performed through the proposed method. Samples containing sparsely distributed single gold nanorods were prepared [16]. The multifocal array with arbitrarily-oriented linear polarization states polarized focal spots are numerically generated in Fig. 2(a) through the phase modulation in Fig. 2(b). With a sharp polarization selectivity of gold nanorods, the characteristic two-photon fluorescence (TPF) intensity patterns can be used for confirmation of the focal polarization states [15, 16]. The orientations of single nanorods are firstly determined by imaging through an azimuthally-polarized beam in Fig. 2(c). The polarization-multiplexed multifocal arrays with desired polarization states can be experimentally confirmed through parallel TPF imaging of gold nanorods in the same area, as shown in Fig. 2(d). As an example, for the y-linearly polarized focal spot, the nanorod “2” aligned along to the y-axis can be excited, but the nanorod “1” aligned orthogonal to the y-axis cannot be excited.

In addition to the individually-controllable polarization state, the multifocal array exhibits sub-diffraction-limited focal field distribution in each focal spot. To verify the sub-diffraction-

limited feature, point spread functions through TPF imaging of single nanorods were obtained and compared to those obtained directly from a linearly-polarized beam without any modulation. Figures 3(a) and 3(b) show the TPF intensity plots of the nanorod excited by the π-PMAB and the linearly-polarized beam along the x-and y-directions, respectively. It is clear to see that the focal spot of the π-PMAB is 10% smaller than the diffraction-limit focal spot of a linearly polarized beam in the full width at half maximum (FWHM), which is reasonably consistent with the Debye calculation.

The demonstrated polarization-multiplexed multifocal array not only provides the sub-diffraction-limited feature but also exhibits high polarization purity for NA objectives due to the depolarization-free nature of our method. To demonstrate this feature, the polarization purity defined as $I_x/(I_x + I_y + I_z)$ within the FWHM confined focal area (the inset of Fig. 3(c)) are numerically investigated for the x-linearly-polarized focal spot derived from a π-PMAB and compared with that obtained from a tightly focused linearly-polarized beam. In Fig. 3(c), the simulation results reveal that high focal polarization purity for objectives with any NA is maintained by the π-PMAB owing to the pure transverse polarization nature of the azimuthally-polarized beam. In contrary, the focal polarization purity of the linearly-polarized beam tends to drop as the NA increases due to the appearance of a longitudinal component induced by the depolarization effect. In particular, in the case of NA=1.4, the linearly-polarized beam is with

13% degraded focal polarization purity compared to the π-PMAB. The high polarization purity is experimentally corroborated by the TPF imaging of a single gold nanorod. The TPF intensity obtained by an objective with NA=0.8 and NA=1.4 at different polarization orientations can be well fitted with a biquadratic cosine curve consistent with the previous report [15], which implies the high polarization purity was achieved in the linearly-polarized focal spot generated from the π-PMAB, as shown in Fig. 3(d).

The demonstrated method can allow for parallel recording of multiple information with different polarization states in the multi-dimensional optical data storage. To achieve the parallel polarization-multiplexed recording, each of the focal spot with a different polarization state can be dynamically switched "on" and "off" corresponding to the spatial binary information flow from each polarization channel, as shown in Fig. 4(a). Gold nanorods dispersed polymer sample was prepared for polarization-multiplexed recording [9, 15]. For multiplexed recording, the pulse energy at a power of 4mW and an exposure time of 25 ms was optimized to eliminate crosstalks between the different polarization channels. Consequently, Fig. 4(b) shows the parallelly-multiplexed patterns can be simultaneously retrieved with the corresponding polarization states.

In conclusion, we have demonstrated a polarization-multiplexed multifocal array with sub-diffraction-limited and high polarization purity features under a high NA objective. With these features, an arbitrarily-oriented linearly-polarized multifocal array has been employed for parallel

polarization-multiplexed optical recording. The demonstrated method advances the multifocal array technique and paves the avenue for a variety of polarization-multiplexed applications such as optical communication [23], polarization-sensitive nanophotonic devices [24], direct laser writing [25, 26], and chiral plasmonics [27, 28].

Acknowledgement:

This work is supported by the Australian Research Council (ARC) Laureate Fellowship scheme (FL100100099).

References

1. R. M. A. Azzam and N. M. Bashara, Ellipsometry and Polarized Light (North-Holland, Amsterdam, 1977).
2. Emil Wolf, "Electromagnetic diffraction in optical systems, I. An integral representation of the image field," Proceedings of the Royal Society. London. **A253**, 349-357 (1959).
3. Min Gu, Advanced Optical Imaging Theory (SpringerVerlag, Heidelberg, 2000).
4. Qiwen Zhan, "Cylindrical vector beams: from mathematical concepts to applications," Advances in Optics and Photonics. **1**, 1-57 (2009).
5. Haifeng Wang, Luping Shi, Boris Lukyanchuk, Colin Sheppard, and Chong Tow Chong, "Creation of a needle of longitudinally polarized light in vaccum using binary optics," Nature Photonics. **2**, 501-505 (2008).
6. Yunshan Jiang, Xiangping Li, and Min Gu, "Generation of sub-diffraction-limited pure longitudinal magnetization by the inverse Faraday effect by tightly focusing an azimuthally polarized vortex beam." Optics Letters. **38**, 2957-2960 (2013).
7. H. J. Simon, and N. Bloembergen, "Second-harmonic light generation in crystals with natural optical activity," Physical Review. **171**, 1104-1113 (1968).
8. KuniakiKonishi, Takuya Higuchi, Jia Li, Jakob Larsson, Shuntaro Ishii, and Makoto Kuwata-Gonokami, "Polarization-controlled circular second-harmonic generation from metal hole arrays with threefold rotational symmetry," Physical Review Letters. **112**, 135502 (2014).
9. Peter Zijlstra, James W. M. Chon, and Min Gu, "Five-dimensional optical recording mediated by surface plasmons in gold nanorods," Nature. **459**, 410-413 (2009).
10. Xiangping Li, Qiming Zhang, Xi Chen, and Min Gu, "Giant refractive-index modulation by two-photon reduction of fluorescent grapheme oxides for multimode optical recording," Scientific Reports. **3**, 2819 (2013).
11. Min Gu, Xiangping Li, and Yaoyu Cao, "Optical storage arrays: a perspective for future big data storage," Light: Science & Applications. **3**: e177 (2014).
12. M. Andreas Lieb, James M. Zavislan, and Lukas Novotny, "Single-molecule orientations determined by direct emission pattern imaging," Journal of the Optical Society of America B. **21**, 1210-1215 (2004).
13. Philip. R. Dolan, Xiangping Li, JelleStorteboom, and MinGu, "Complete determination of the orientation of NA centers with radially polarized beams,"Optics Express. **22**, 4379-4387 (2014).
14. Max Born, and Emil Wolf, Principles of Optics: Electromagnetic Theory of Propagation, Interference, and Diffraction of Light 7th edition (Cambridge University Press, Cambridge, UK, 1999).

15. Xiangping Li, Tzu-Hsiang Lan, Chung-HaoTien, and Min Gu, "Three-dimensional orientation-unlimited polarization encryption by a single optically configured vectorial beam," Nature Communication. **3**, 998 (2012).
16. Min Gu, Han Lin, and Xiangping Li, "Parallel multiphoton microscopy with cylindrically polarized multifocal arrays," Optics Letters. **38**, 3627-3630 (2013).
17. Han Lin, and Min Gu, "Creation of diffraction-limited non-Airy multifocal arrays using a spatially shifted vortex beam," Applied Physics Letters. **102**, 084103 (2013).
18. Alexander Jesacher, and Martin J. Booth, "Parallel direct laser writing in three dimensions with spatially dependent aberration correction," Optics Express. **18**, 21090-21099 (2010).
19. Haoran Ren, Han Lin, Xiangping Li, and Min Gu, "Three-dimensional parallel recording with a Debye diffraction-limited and aberration-free volumetric multifocal array," Optics Letters. **39**, 1621-1624 (2014).
20. Xiangping Li, Priyamvada Venugopalan, Haoran Ren, and Min Gu, "Super-resolved pure-tansverse focal fields with an enhanced energy density by focusing an azimuthally polarized first-order vortex beam," Optics Letters. accepted.
21. Svetlana N. Khonina, and Ilya Golub, "Optimization of focusing of linearly polarized light," Optics Letter. **36**, 352-354 (2011).
22. Roberto Di Leonardo, Francesca Ianni, and Giancarlo Ruocco, "Computer generation of optimal holograms for optical trap arrays," Optics Express. **15**, 1913-1922 (2007).
23. Jian Wang, Jeng-Yuan Yang, Irfan M. Fazal, Nisar Ahmed, Yan Yan, Hao Huang, Yongxiong Ren, Yang Yue, Samuel Dolinar, Moshe Tur, and Alan E. Willner, "Terabit free-space data transmission employing orbital angular momentum multiplexing," Nature Photonics. **6**, 488-496 (2012).
24. Xiangping Li, James W. M. Chon, Richard A. Evans, and Min Gu, "Quantum-rod dispersed photopolymers for multi-dimensional photonic applications," Optics Express. **17**, 2954-2961 (2009).
25. Zongsong Gan, Yaoyu Cao, Richard A. Evans, and Min Gu, "Three-dimensional deep sub-diffraction optical beam lithography with 9nm feature size," Nature Communication. **4**, 2061 (2013).
26. Martti Silvennoinen, Jarno Kaakkunen, Kimmo Paivasaari and Pasi Vahimaa, Optics Express. **22**, 2603-2608 (2014).
27. Wei Ma, HuaKuang, Libing Wang, LiguangXu, Wei-Shun Chang, Huanan Zhang, Maozhong Sun, Yinyue Zhu, Yuan Zhao, Liqiang Liu, ChuanlaiXu, Stephan Link, and Nicholas A. Kotov, "Chiral plasmonics of self-assembled nanorod dimers," Scientific Reports. **3**, 1934 (2013).

28. Mark D. Turner, Matthias Saba, Qiming Zhang, Benjamin P. Cumming, Gerd E. Schroder-Turk, and Min Gu, “Miniature chiral beamsplitter based on gyroid photonic crystals,” Nature Photonics. **7**, 801-805 (2013).

Fig. 1. The intensity distributions in the focal plane of an azimuthally-polarized beam (a) and a π-PMAB (b), dashed line indicates the orientation of the phase-step line. (c) Experimental configuration for generating a multifocal array with an arbitrarily-orientated linear polarization states under a high NA objective. SLM: spatial light modulator, APC: azimuthal polarization converter.

Fig. 2. The intensity distributions (a) and its phase modulation (b) of a polarization-multiplexed multifocal array with an arbitrarily-orientated linear polarization states. (c) TPF imaging of gold nanorods illuminated by an azimuthally-polarized beam and the orientations of eight nanorods are labeled from“1” to “8”. (d) Parallel TPF imaging within the same area using the polarization-multiplexed multifocal array.

Fig. 3. The comparison of TPF intensity plots of a single nanorod excited by the π-PMAB and by the linearly-polarized beam along the x- (a) and y- (b) directions, respectively. (c) The comparison of focal polarization purity between the π-PMAB and the linearly-polarized beam for different NAs. The inset shows the FWHMs defined area. (d) Normalized TPF intensity from single gold nanorods excited by the π-PMAB foci with a $\pi/10$ piecewise orientation shifting under an objective of NA=0.8 and NA=1.4, respectively.

Fig. 4. (a) A schematic illustration of the parallel polarization-multiplexed recording wherein four polarization channels with different patterns are parallelly recorded. The black wave-shapes illustrate the information flows of four polarization channels. (b) The parallelly-multiplexed patterns are simultaneously retrieved with the corresponding polarization states.

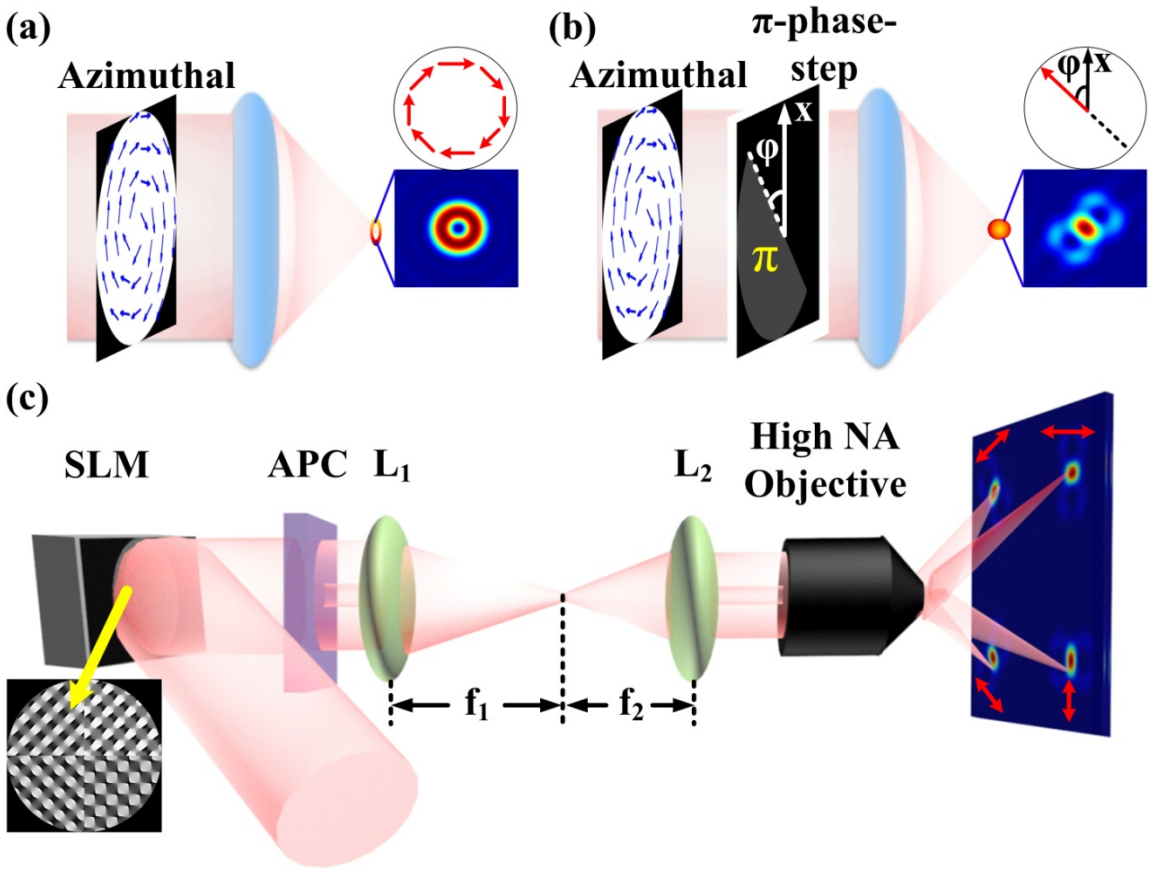
(a)
Azimuthal
(b)
Azimuthal
π-phase-step
x
φ
π
φ
x
(c)
SLM
APC
L1
L2
High NA Objective
f1
f2

Fig. 1

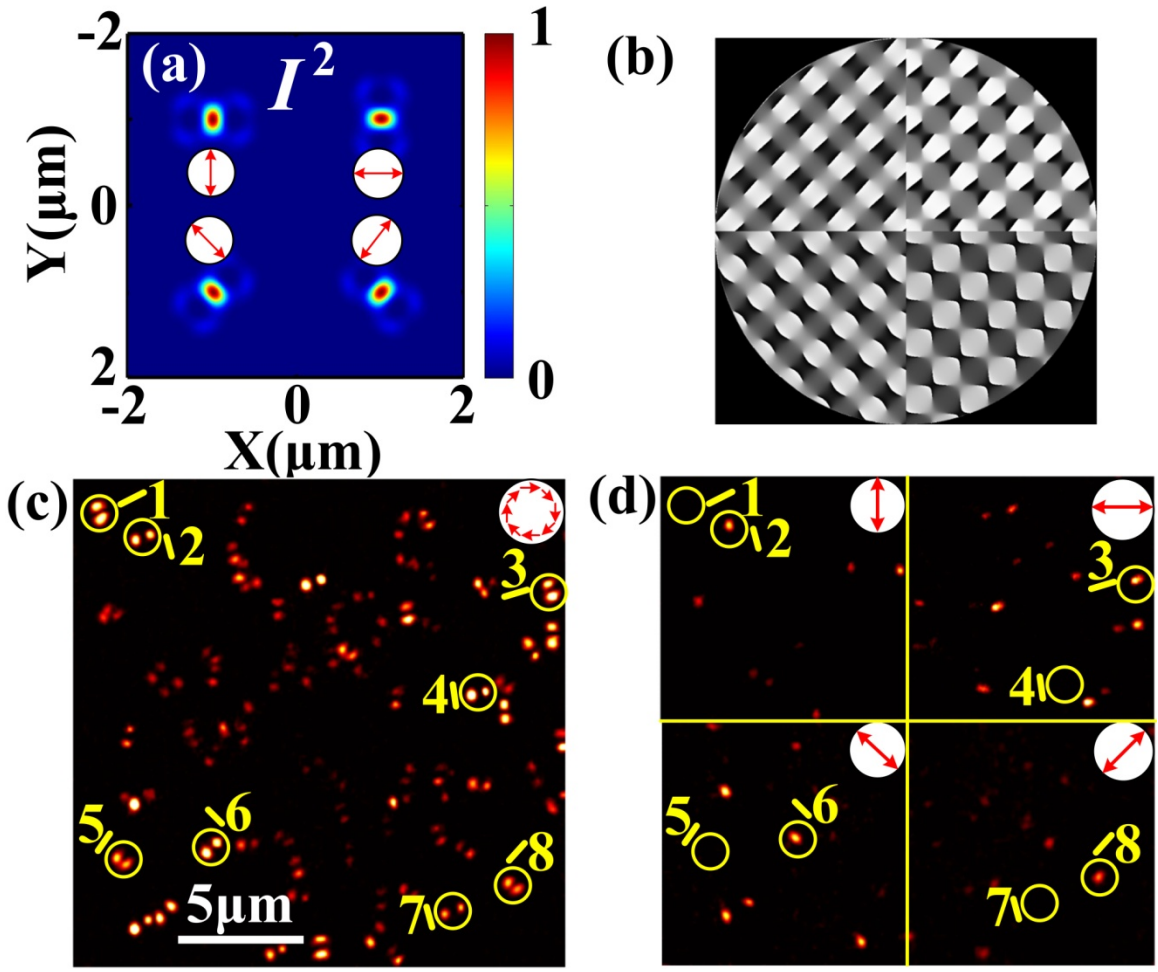

Fig. 2

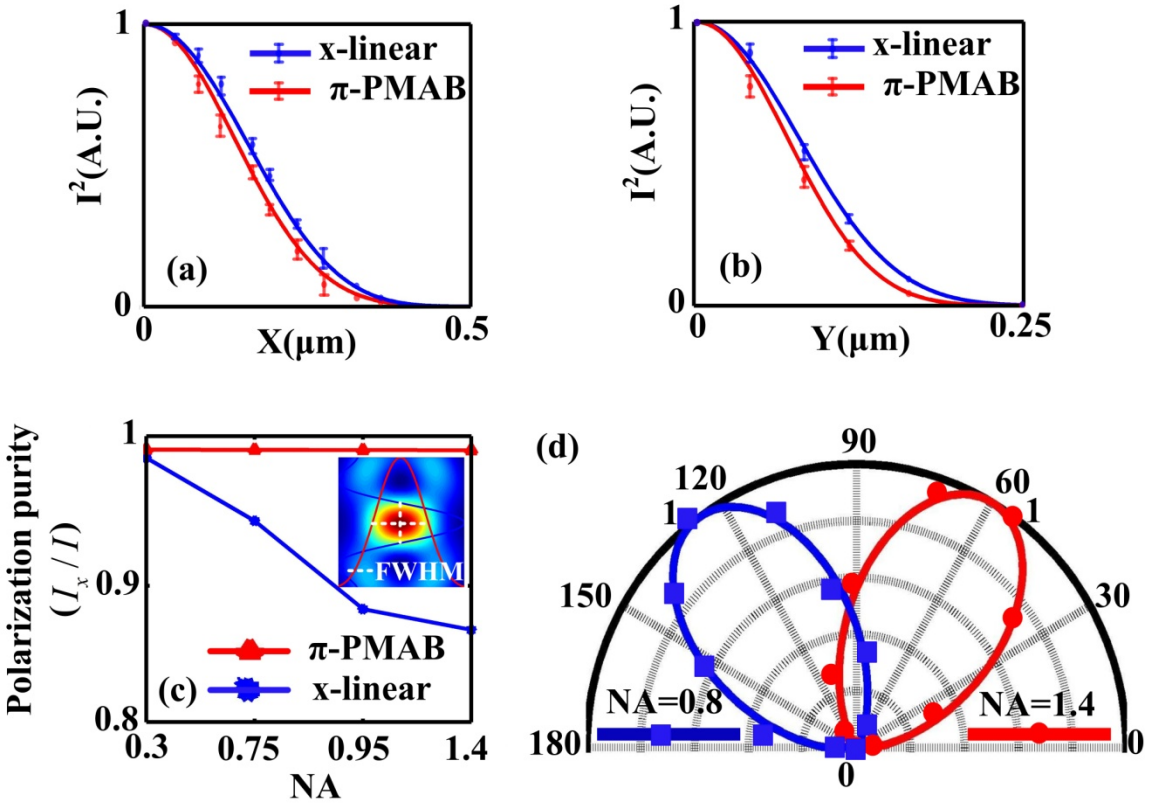
1
0
I²(A.U.)
x-linear
π-PMAB
(a)
0
X(μm)
0.5
(b)
Y(μm)
0.25
Polarization purity
(I_x / I)
0.9
0.8
FWHM
(c)
0.3
0.75
0.95
1.4
NA
(d)
90
120
60
150
30
180
NA=0.8
NA=1.4

Fig. 3

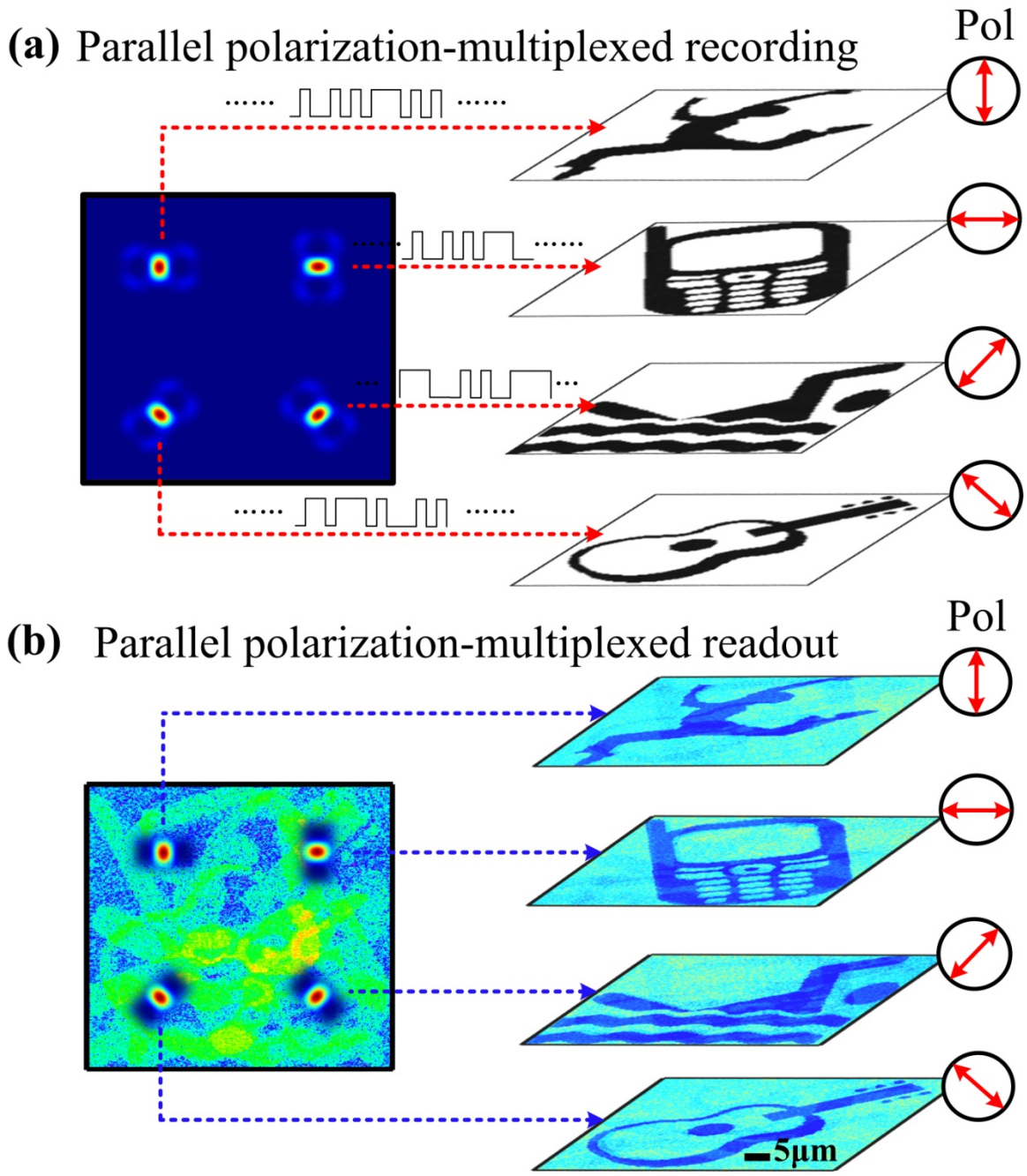
(a) Parallel polarization-multiplexed recording
Pol
(b) Parallel polarization-multiplexed readout
Pol
5μm

Fig. 4